

Q-Learning Algorithm for VoLTE Closed-Loop Power Control in Indoor Small Cells

Faris B. Mismar and Brian L. Evans

Wireless Networking and Communications Group, The University of Texas at Austin, Austin, TX 78712 USA

Abstract—We propose a closed-loop power control algorithm for the downlink of the voice over LTE (VoLTE) radio bearer for an indoor environment served by small cells. The main contributions of our paper are: 1) proposing closed-loop power control for downlink VoLTE (or any packetized voice bearer), 2) deriving an upper bound of the loss in VoLTE downlink signal to noise plus interference ratio which the closed-loop power control has to overcome, 3) employing reinforcement learning to perform closed-loop power control, and 4) showing that this closed-loop power control method can improve the quality of VoLTE in a realistic network setup. Our simulation results have shown that our proposed algorithm significantly improved both voice retainability and mean opinion score as a result of maintaining the effective downlink signal to interference plus noise ratio against adverse network operational issues and faults.

Index Terms—reinforcement learning, artificial intelligence, VoLTE, MOS, QoE, optimization, SON.

I. INTRODUCTION

Wireless networks are vulnerable to operational issues and faults. While some services are more resilient against wireless link faults by means of retransmissions and robust modulation and coding, other services—such as voice—cannot benefit from retransmission and must be made robust against faults through other means. The received *signal to interference plus noise ratio* (SINR) is a critical quantity to ensure resilient communications in applications such as *voice over LTE* (VoLTE). In this regard, we adopt reinforcement learning to improve downlink SINR (DL SINR) in a VoLTE call. In our case, network issues and faults reduce the effective downlink SINR. The power control reinforcement learning agent strives to improve it through power control commands. We propose actions based on tabular *Q*-Learning.

Downlink closed-loop power control is last implemented in 3G *universal mobile telecommunications system* (UMTS) [1]. It rapidly adjusts the transmit power of a radio link of a dedicated traffic channel to match the target DL SINR. This technique is not present in 4G LTE or 5G due to the absence of dedicated traffic channels for packet data sessions. However, the introduction of *semi-persistent scheduling* (SPS) in 4G LTE has created a virtual sense of a dedicated downlink traffic channel for VoLTE on which a closed-loop power control can be performed. This scheduling is at least for the length of one voice frame—which is in order of tens of LTE *transmit time intervals* (TTIs).

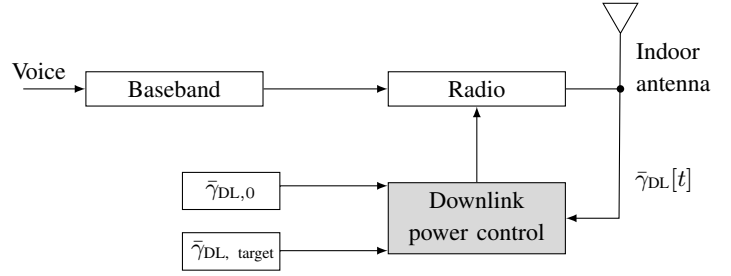


Fig. 1. Downlink power control module. $\bar{\gamma}[t]$ is the effective signal to noise plus interference ratio (SINR) at the receiver at time t fed back to the downlink power control module, which has to maintain the downlink SINR at the receiver at $\bar{\gamma}_{DL, target}$.

In this paper, we therefore propose optimizing the effective downlink SINR measured at the receiver ($\bar{\gamma}_{DL}$) using *power commands* (PCs), allowing the pre-existing *adaptive modulation and coding* (AMC) to perform in a region of an improved target SINR if feasible. This improved target SINR ($\gamma_{target, DL}$) is an input to our *Q*-Learning closed-loop power control algorithm as shown in Fig. 1.

For this purpose, we model a cellular cluster of low power base stations in an indoor environment operating in a typical sub-6 GHz frequency range—in resemblance to 4G LTE networks today—with mobile devices scattered in the vicinity and adjacent small cells acting as interferers. We refer to any of these mobile devices or VoLTE capable smartphones as a *user equipment* (UE). The effective downlink SINR is reported by the UEs back to the base station on the uplink. We chose to treat interference from these surrounding cells as noise. This is a justified assumption in [2] and is a baseline practice. While the noise distribution may not be Gaussian due to the dominance of the interfering cell, the Gaussian channel is the lower bound of capacity calculations [3], and therefore is our choice.

While the focus of our paper is on VoLTE, we believe any future technology that offers packetized voice can benefit from this algorithm. In fact, with the highly anticipated role of *self-organizing networks* (SON) in 5G [4], we believe that the introduction of DL SINR for voice services improving the mmWave coverage against network impairments is a significant contribution towards machine learning enabled SON.

The authors in [5] used an improved decentralized

Q-Learning algorithm to reduce interference in the LTE femtocells environment. They compared their approach with various power control algorithms including open loop power control. There was no reference to closed-loop power control, which we propose.

Combining information theory with machine learning, the authors [6] proposed a deep reinforcement learning method which maximizes the *Q*-function using the Kullback-Leibler (KL) divergence and entropy constraints instead of the exploration, which we used in this paper. They used a stochastic Gaussian policy and solved a constrained optimization problem in a closed form for a special case.

In [7], the authors proposed a closed-loop power control implementation for LTE and used fractional path loss compensation and improved the system performance. No machine learning was used and no downlink power control was proposed.

The authors of [8] performed *Q*-Learning based power control for indoor LTE femtocells with an outdoor macro cell but had a focus on throughput. They relied on the UE reported SINR or call quality indicator to change the femtocell transmit power. They introduced a central controller to resolve the issue of communicating base stations. We confined the geographical area to make it feasible for the base stations to communicate through the backhaul. The paper also assumed that downlink power control is achieved over shared data channels, which is a relaxed assumption and requires that the scheduler is aware ahead of time about the channel condition for the upcoming user to perform power control.

All papers [5], [7], [8] addressed the area of LTE and either machine learning or power control, but none used the downlink power control for the traffic channels held for the duration of a VoLTE call, which is the essence of our contribution in this paper.

Our main contributions are as follows:

- 1) Propose closed-loop power control for downlink VoLTE (or any other packetized voice bearer).
- 2) Derive an upper bound of the loss in VoLTE DL SINR which the closed-loop power control has to overcome.
- 3) Employ reinforcement learning to perform closed-loop power control.
- 4) Show that this closed-loop power control method can improve the quality of VoLTE in a realistic network setup.

II. SYSTEM MODEL

The system comprises two components:

- 1) A radio environment where VoLTE capable UEs are served.
- 2) A reinforcement learning model using *Q*-Learning to perform closed-loop power control to improve effective DL SINR measured at the receiver.

A. Radio Environment

The radio environment is an indoor cellular cluster with one tier of neighboring small cells each with a square

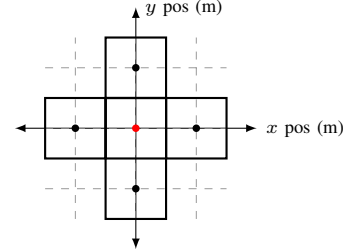


Fig. 2. Radio environment. The red point represents the serving cell. The black points in the adjacent squares are the low power nodes.

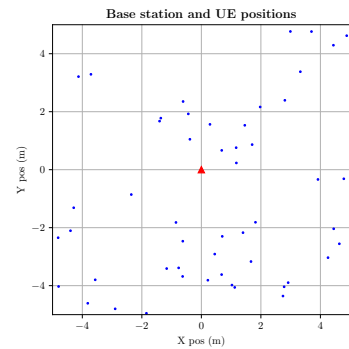


Fig. 3. The serving cell layout. The serving cell is the red triangle and user equipment (UEs) are randomly scattered in blue.

geometry length L as shown in Fig. 2. The UEs are scattered in \mathbb{R}^2 according to a *homogeneous poisson point process* (PPP) [9]. This process Φ has an *intensity parameter* λ which represents the expected number of users served by the small cell per unit area. We define the point process Φ by the number of users N in the service area of the small cell W sampled from a Poisson distribution with mean $\lambda W = \lambda L^2$. The i -th UE position is i.i.d. sampled from a continuous uniform distribution as in Fig. 3.

We chose the square geometry because in an indoor environment with a typical omnidirectional cell installed at the center of square-shaped floor plans, a square tessellation is possible. This is because as the transmitted signals are attenuated further more towards the square forming walls. In practice, square geometry has been used in indoor commercial deployments [10], and is therefore our choice.

This cellular cluster can be in a normal state or undergo some fault-generating actions. To increase the complexity of the implementation, we add alarm recovery to the cluster which clears the alarm after it happening with a given probability as in Table I, resembling what live networks have.

Our link budget at any TTI t is written in dBm as:

$$P_{\text{UE},i}[t] = P_{\text{TX},i}[t] + G_{\text{TX}} - L_{\text{m}} - L_{\text{a}} + G_{\text{UE}} + 10 \log G_{\text{div}} \quad (1)$$

where $P_{\text{UE},i}$ is the received power for the allocated *physical resource blocks* (PRB) transmitted at power P_{TX} , G_{TX} is the antenna gain of the transmitter, L_{m} is a miscellaneous loss (e.g., feeder loss and return loss), L_{a} is the path loss over

TABLE I
NETWORK ACTIONS

Action ν	Definition	Probability
0	Cluster is normal.	p_0
1	Feeder fault alarm (3 dB loss of signal).	p_1
2	Neighboring cell down.	p_2
3	VSWR out of range alarm.	p_3
4	Feeder fault alarm cleared. [†]	p_4
5	Neighboring cell up again. [†]	p_5
6	VSWR back in range. [†]	p_6

[†] These actions cannot happen if their respective alarm did not happen first.

the air interface for line of sight indoor propagation, and G_{UE} is the UE antenna gain. G_{div} is the transmit diversity gain which cannot exceed the number of data streams.

We compute the received SINR for the i -th UE at TTI t ($\gamma_{\text{DL},i}[t]$) as:

$$\gamma_{\text{DL},i} \triangleq \frac{P_{\text{UE},i}}{N + \sum_{j: \mathbf{o}_j \in \Theta \setminus \{\mathbf{o}_0\}} P_{\text{UE},j}}, \quad i = \{1, 2, \dots, N_{\text{UE}}\} \quad (2)$$

we dropped the time for ease of notation. N is the noise sampled from a zero-mean Normal distribution with variance equal to the noise power, $P_{\text{UE},i}$ is defined as in (1). Θ is a set of all the cells in the cluster and \mathbf{o}_j is the coordinates of the j -th base station ($j = 1, 2, 3, 4$).

Now we can write the *effective downlink SINR at the receiver* at a given TTI t , $\bar{\gamma}_{\text{DL}}[t]$ as:

$$\bar{\gamma}_{\text{DL}}[t] \triangleq 10 \log \left(\frac{1}{N_{\text{UE}}} \times \sum_{i=1}^{N_{\text{UE}}} \gamma_{\text{DL},i}[t] \right) \quad (\text{dB}) \quad (3)$$

which is the quantity that the *power control* (PC) has to improve.

B. Reinforcement Learning

We used tabular *Q*-Learning [11] to implement the closed-loop PC. One episode z of reinforcement learning has the duration of one VoLTE frame (20 TTIs). We have a maximum of ζ^* episodes corresponding to ζ^* VoLTE frames.

The set of states in which our closed-loop PC algorithm (Algorithm 1) can be is denoted as \mathcal{S} and set of PC actions is \mathcal{A} . The set of rewards is denoted as \mathcal{R} . These elements are in Fig. 4. We show the *Markov decision process* (MDP) for these elements of reinforcement learning in the steady state in Fig. 5. The *stochastic policy* at time t is defined with respect to an action $a \in \mathcal{A}$ and a state $s \in \mathcal{S}$ as [11]:

$$\pi(a|s) \triangleq \mathbb{P}[A(t) = a | S(t) = s] \quad (4)$$

The *reward* at a given TTI t is a number denoted by $r_{s,a}[t] \in \mathcal{R}$ and is a result of the action $a \in \mathcal{A}$ taken by the

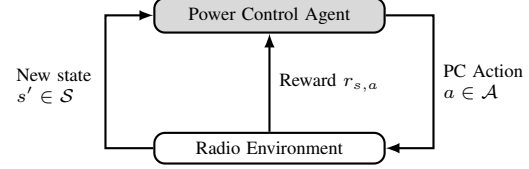


Fig. 4. Reinforcement learning elements.

agent and moved to the state $s \in \mathcal{S}$. The reward is:

$$r_{s,a}[t] \triangleq \begin{cases} -\infty, & \gamma_{\text{DL}}[t] = \gamma_{\text{DL, target}} \text{ is met with } t \ll \tau \\ -5, & \gamma_{\text{DL, target}} \text{ is not feasible} \\ -1, & \gamma_{\text{DL}}[t] < \gamma_{\text{DL}}[t-1] \\ 0, & \gamma_{\text{DL}}[t] = \gamma_{\text{DL}}[t-1] \\ +1, & \gamma_{\text{DL}}[t] > \gamma_{\text{DL}}[t-1] \\ +2, & \gamma_{\text{DL}}[t] = \gamma_{\text{DL, target}} \text{ is met} \end{cases} \quad (5)$$

where $\gamma_{\text{DL, target}}$ is a finite improvement Δ_γ over the initial DL SINR owed to the closed-loop PC algorithm ($\gamma_{\text{DL, target}} \triangleq \Delta_\gamma + \gamma_{\text{DL, 0}}$).

PC actions are listed in Table II. The PC algorithm attempts to reach $\bar{\gamma}_{\text{DL, target}}$ through a series of PC contributions $\delta(\cdot; t)$ in reaction to various radio losses from the network during any given TTI t :

$$\begin{aligned} a &= \arg \max_{a'} Q(s, a') \\ \Delta_\gamma(\tau) &\triangleq \sum_{t=1}^{\tau} \delta(a \in \mathcal{A}; t) \cdot \mathbb{P}[a \in \mathcal{A}; t] - \\ &\quad \delta(\nu \in \mathcal{N}; t) \cdot \mathbb{P}[\nu \in \mathcal{N}; t] \end{aligned} \quad (6)$$

where $\delta(a \in \mathcal{A}; t)$ is the SINR gain (or loss) as a result of the PC action a from Table II during TTI t , and $\delta(\nu \in \mathcal{N}; t)$ is a result of network actions from Table I. The probability of occurrences and $\mathbb{P}[a \in \mathcal{A}; t]$ are both computed over TTI t . Here we show the computations of the actions $\nu \in \mathcal{N}$ taken by the network and their impact on the downlink SINR contribution $\delta(\nu \in \mathcal{N}; t) \triangleq \bar{\gamma}_{\text{DL}}[t] - \bar{\gamma}_{\text{DL}}[t-1]$.

Computation of contribution of actions $\nu = 1, 3$. When the voltage standing wave ratio (VSWR) changes from v_0 to v in TTI t , we compute the change in loss due to return loss as:

$$\Delta L = 10 \log \left(\left| \frac{v_0 + 1}{v_0 - 1} \right| \cdot \left| \frac{v - 1}{v + 1} \right| \right)^2 \quad (7)$$

Now compute the SINR gain (or loss) as $\delta(\nu \in \mathcal{N}; t) = \bar{\gamma}_{\text{DL}}[t-1] + \Delta L$. Action $\nu = 1$ is a special case with $\Delta L = -3 \text{ dB}$.

Computation of contribution of action $\nu = 2$. When the neighbor cell k is down, the transmit power of the adjacent cells j will increase by an arbitrary quantity $0 < \varepsilon_j \leq 1$ and the number of interferers will decrease. Therefore, we

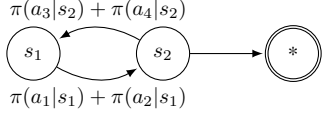


Fig. 5. The steady state Markov decision process $(\mathcal{S}, \mathcal{A}, \mathcal{R}, \pi(\cdot | \cdot), \gamma)$ used by the Q -Learning model. $\pi(\cdot | \cdot)$ is the conditional transitional probability.

TABLE II
POWER CONTROL (PC) ALGORITHM ACTIONS AT TIME t

Action a	Definition
0	Nothing (this is a transient action).
1	Decrease transmit power $P_{\text{TX}}[t]$ by $\delta(a; t) = -3$ dB.
2	Decrease transmit power $P_{\text{TX}}[t]$ by $\delta(a; t) = -1$ dB.
3	Increase transmit power $P_{\text{TX}}[t]$ by $\delta(a; t) = 1$ dB.
4	Increase transmit power $P_{\text{TX}}[t]$ by $\delta(a; t) = 3$ dB.

TABLE III
POWER CONTROL (PC) ALGORITHM STATES

State s	Definition
0	No PC issued.
1	PC = 1 (Actions $a \in \{3, 4\}$ have been played).
2	PC = 0 (Actions $a \in \{1, 2\}$ have been played).

can write the upper bound of the SINR loss $\delta(\nu \in \mathcal{N}; \tau)$ as:

$$\begin{aligned} \delta(\nu \in \mathcal{N}; \tau) &= \frac{P_{\text{UE},0}}{N + \sum_{j:r_j \in \Theta \setminus \{\mathbf{o}_0\}} P_{\text{UE},j}} \\ &\stackrel{(a)}{\geq} \frac{P_{\text{UE},i}}{N + \sum_{j \neq k: r_j \in \Theta \setminus \{\mathbf{o}_0\}} (1 + \varepsilon_j) P_{\text{UE},j}} \\ &\stackrel{(b)}{\geq} \frac{P_{\text{UE},i}}{N + |\Theta \setminus \{\mathbf{o}_0, \mathbf{o}_k\}| \cdot P_{\text{LPN, max}}} \\ &\stackrel{(c)}{=} \frac{P_{\text{UE},i}}{N + (|\Theta| - 2) \cdot P_{\text{LPN, max}}} \end{aligned} \quad (8)$$

where (a) is since the denominator increased by a positive quantity. (b) is true because we use the maximum small cell transmit powers instead of the increased received power measured at the UE. (c) is since the cardinality of Θ is reduced by two: the serving cell 0 and the neighbor k from step (b).

We define the *optimal action-value function* $Q^*(s, a)$ as:

$$Q^*(s, a) \triangleq \mathbb{E}_{s'} \left[r_{s,a} + \gamma \max_{a'} Q^*(s', a') \mid s, a \right] \quad (9)$$

where s' and a' are the next state and next action [11]. The action a and state s is a PC action and state from Tables II and III respectively.

III. POWER CONTROL ALGORITHMS

A. Fixed Power Allocation

The *fixed power allocation* (FPA) power control method is an open-loop PC algorithm. This open-loop PC algorithm is our baseline algorithm for performance benchmarking

Algorithm 1 VoLTE Downlink Closed-Loop Power Control

Input: Initially computed effective downlink SINR value ($\bar{\gamma}_{\text{DL},0}$) and desired target effective SINR value ($\bar{\gamma}_{\text{DL, target}}$).
Output: Optimal sequence of power commands required to achieve the target SINR value during a VoLTE frame z , which has a duration of τ .

- 1: Define the set of power control (PC) actions \mathcal{A} , the set of PC states \mathcal{S} , the exploration rate ϵ , the decay rate d , and ϵ_{\min} . Tables II, III, and V give example values for these terms.
- 2: $t \leftarrow 0$ ▷ Initialize time
- 3: $\bar{\gamma}_{\text{DL}} \leftarrow \bar{\gamma}_{\text{DL},0}$ ▷ Initialize effective downlink SINR
- 4: $(s, a) \leftarrow (0, 0)$ ▷ Initialize actions and states
- 5: **repeat**
- 6: $t \leftarrow t + 1$ ▷ Next transmit time interval
- 7: $\epsilon \leftarrow \max(\epsilon \cdot d, \epsilon_{\min})$ ▷ Decay exploration rate
- 8: Sample $r \sim \text{Uniform}(0, 1)$
- 9: **if** $r \leq \epsilon$ **then**
- 10: Select an action $a \in \mathcal{A}$ at random.
- 11: **else**
- 12: Select an action $a \in \mathcal{A}$, $a = \arg \max_{a'} Q(s, a')$.
- 13: **end if**
- 14: Perform action a (power control) and obtain reward $r_{s,a} \in \mathcal{R}$ from (5).
- 15: Base station to increase $\bar{\gamma}_{\text{DL}}$ by increasing $P_{\text{TX}}[t]$ by $\delta(a; t)$ from Table II using (11).
- 16: Observe next state s' .
- 17: Update the table entry $Q(s, a)$ as in (9).
- 18: $s \leftarrow s'$
- 19: **until** $\bar{\gamma}_{\text{DL}} \geq \bar{\gamma}_{\text{DL, target}}$ or $t \geq \tau$

purposes. It is a common power allocation scheme where the total transmit power is simply divided equally among all PRBs in the operating band N_{PRB} and is therefore constant but cannot exceed the maximum transmission power of the small cell:

$$P_{\text{TX}}[t] \triangleq P_{\text{LPN, max}} - 10 \log N_{\text{PRB}} \quad (\text{dBm}) \quad (10)$$

B. Closed-Loop Power Control

Owed to the closed-loop PC, we can write P_{TX} at any given TTI t as:

$$P_{\text{TX}}[t] = \min (P_{\text{LPN, max}}, P_{\text{TX}}[t-1] + \eta[t] (\mathbb{1}_{\text{PC}[t]=1} - \mathbb{1}_{\text{PC}[t]=0})) \quad (\text{dBm}) \quad (11)$$

where $\mathbb{1}_{(\cdot)}$ is the indicator function and $\eta[t]$ is the repetition count of a power command in a given TTI t as in Table II. Power control cannot cause the transmit power to exceed the maximum transmit power of the serving cell.

From a time complexity perspective, we observe that for FPA, the open-loop PC only sets the transmit power once at call establishment and responds to alarms or clearing of alarms, therefore it has a time complexity in $\mathcal{O}(1)$. For the closed-loop PC algorithm, the the upper bound of the time complexity for Q -Learning is in $\mathcal{O}(n^2)$ [12], with $n \triangleq |\mathcal{S}|$.

IV. VOICE CALL QUALITY BENCHMARK

We we used two performance metrics: *call retainability* and *mean opinion score* (MOS) to compare both algorithms.

A. Voice Retainability

We define voice retainability for the radio environment as a function of an effective downlink SINR threshold γ_0 :

$$\text{Retainability} \triangleq 1 - \frac{1}{\tau \zeta^*} \sum_{z=0}^{\zeta^*} \sum_{t=0}^{\tau} \mathbb{1}_{\bar{\gamma}[t; z] \leq \gamma_0} \quad (12)$$

where ζ^* is the optimal episode for which the simulation is running and $\bar{\gamma}[t; z]$ is $\bar{\gamma}[t]$ obtained during episode $z : 0 < z \leq \zeta^*$.

B. Mean-Opinion Score

To benchmark the audio quality, we computed *mean-opinion score* (MOS) using the experimental MOS formula [13]. We obtained the packet error rate from the simulation over τ frames in the optimal episode ζ^* using the symbol probability of error of a QPSK modulation in OFDM [14]. We chose a VoLTE data rate of 23.85 kbps and a voice activity factor (ratio of voice payload to silence during a voice frame) of 0.7. We refer to the source code [15] for further details. Result is in Fig. 9.

V. SIMULATION RESULTS

We implemented Algorithm 1 using Python and Keras [16]. Keras provides an extra layer of usability with TensorFlow [17] as a backend. We set the machine learning parameters as in Table V.

We set the probabilities in Table I as: $p_0 = 5/11, p_1 = p_2 = p_3 = \dots = p_6 = 6/11$. This way we give all faults an equally likely chance of occurrence while having the network perform reliably at least for 45% of the time. For the retainability, we chose $\gamma_0 = 0$ dB in (12). The radio network parameters are set as in Table IV. We further set $\bar{\gamma}_{\text{DL},0}$ to 4 dB, $\bar{\gamma}_{\text{DL},\text{target}}$ to 6 dB, and $\bar{\gamma}_{\text{DL},\text{min}}$ to -3 dB.

In the initial episodes with $\epsilon \sim 1$, closed-loop may perform worse than FPA. However, as $\epsilon \sim \epsilon_{\min}$, the optimal *Q*-Learning action-value function (9) is learned and the closed-loop PC performs better than FPA. We refer to the source code [15] for further implementation details. Fig. 6 shows the power command sequence for the optimal episode ζ^* , where the closed-loop PC algorithm has caused the base station to raise its transmit power consistently (with the exception of one decrease) to meet the desired DL SINR target, unlike FPA where no power commands are sent.

Fig. 7 shows both algorithms for an early arbitrary episode ($z = 2$). Here, both closed-loop and open-loop PC failed to meet the target DL SINR within the allocated frame τ as mentioned earlier. Next, we show the same algorithms in Fig. 8 for the final episode ζ^* . The closed-loop PC pushes the effective DL SINR to the target through an optimal sequence of power commands. The improved retainability and empirical MOS scores due to the closed-loop power control algorithm are shown in Table VI and Fig. 9 respectively. The reason why retainability and MOS have improved is understood directly from the impact of the effective DL SINR which increases the quantity of (12) and



Fig. 6. Power controls (PCs) sequence during the optimal episode. Unlike fixed power allocation (FPA), closed-loop power control using Q-Learning (CL) sent several PCs per transmit time interval (TTI) for the entire VoLTE frame.

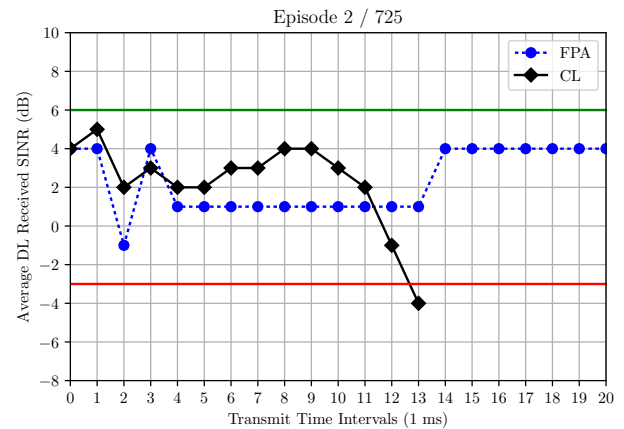


Fig. 7. Downlink signal to interference plus noise ratio (DL SINR) improvement vs. simulation time for both closed-loop power control using *Q*-Learning (CL) and fixed power allocation (FPA) for an arbitrary episode. Green and red lines are $\bar{\gamma}_{\text{DL},\text{target}}$ and $\bar{\gamma}_{\text{DL},\text{min}}$ respectively. CL algorithm ($\epsilon = 0.980$) misses the target and drives DL SINR worse than the minimum while FPA maintains the DL SINR at a higher level.

decreases the packet error rate—the main component in the empirical MOS formula.

VI. CONCLUSION

We introduced downlink closed-loop power control using *Q*-learning, which improved VoLTE performance in an indoor environment compared to the open-loop fixed power allocation power control with alarm recovery. It resulted in a high gain in the quality of experience measured by the voice call retainability and MOS metrics. This is due to the robustness of maintaining the target DL SINR value against the proposed realistic fault scenarios. The ability to maintain this target DL SINR helps maintain a voice call from dropping and reduces the number of voice packets that are in error. We believe that this algorithm can be extended

TABLE IV
RADIO ENVIRONMENT PARAMETERS

Parameter	Value	Parameter	Value
LTE bandwidth	20 MHz	Base station maximum power $P_{LPN, max}$	33 dBm
Downlink center frequency	2.6 GHz	Base station initial power setting	13 dBm
LTE cyclic prefix N_{CP}	normal	Antenna model	omnidirectional
Number of physical resource blocks N_{PRB}	100	Antenna gain G_{TX}	4 dBi
Cellular geometry	square ($L = 10$ m)	Antenna height h_A	10 m
Propagation model	COST 231	User Equipment (UE) antenna gain	-1 dBi
Propagation environment	indoor	UE height h_r	1.5 m
Number of transmit branches N_T	2	Maximum number of UEs per serving cell N_{UE}	10
Number of receive branches N_R	2	UE average movement speed	0 km/h

TABLE V
MACHINE LEARNING PARAMETERS

Parameter	Value
Optimal episode ζ^*	725
One episode duration τ (ms)	20
Gamma γ	0.950
Epsilon ϵ	1.000
Epsilon minimum ϵ_{min}	0.010
Epsilon decay d	0.99
Learning rate	0.001
Number of states	3
Number of actions	5

TABLE VI
RETAINABILITY

Fixed Power Allocation	Closed-loop Q -Learning
47.33%	80.34%

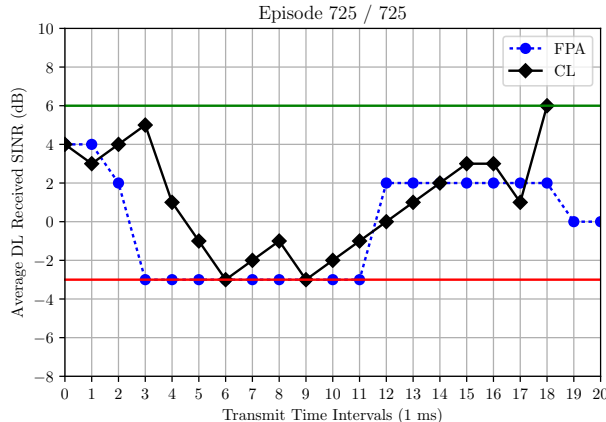


Fig. 8. Downlink signal to interference plus noise ratio (DL SINR) improvement vs. simulation time for both closed-loop power control using Q -Learning (CL) and fixed power allocation (FPA) for the final episode. Green and red lines are $\bar{\gamma}_{DL, target}$ and $\bar{\gamma}_{DL, min}$ respectively. CL algorithm ($\epsilon = \epsilon_{min} = 0.010$) reaches the target while FPA does not.

to any environment or packetized voice technology other than 4G LTE such as 5G or beyond.

REFERENCES

- [1] 3GPP, "Evolved Universal Terrestrial Radio Access (E-UTRA); Physical layer procedures," 3rd Generation Partnership Project (3GPP), TS 25.214, Dec. 2015. [Online]. Available: <http://www.3gpp.org/dynareport/25214.htm>
- [2] M. S. Alouini and A. J. Goldsmith, "Area spectral efficiency of cellular mobile radio systems," *IEEE Trans. on Veh. Tech.*, Jul 1999.
- [3] T. Cover and J. Thomas, *Elements of Information Theory*, 2006.
- [4] A. Imran, A. Zoha, and A. Abu-Dayya, "Challenges in 5G: how to empower SON with big data for enabling 5G," *IEEE Net.*, Nov 2014.
- [5] M. Simsek, A. Czylwik, A. Galindo-Serrano, and L. Giupponi, "Improved decentralized Q -learning algorithm for interference reduction in LTE-femtocells," in *IEEE Wireless Advanced*, June 2011.
- [6] V. Tangkaratt, A. Abdolmaleki, and M. Sugiyama, "Deep Reinforcement Learning with Relative Entropy Stochastic Search," May 2017. [Online]. Available: <https://arxiv.org/abs/1705.07606>
- [7] B. Muhammad and A. Mohammed, "Uplink closed loop power control for LTE system," in *Proc. Int. Conf. on Emerging Tech.*, 2010.
- [8] Z. Gao, B. Wen, L. Huang, C. Chen, and Z. Su, "Q-learning-based power control for lte enterprise femtocell networks," *IEEE Systems Journal*, vol. 11, no. 4, Dec 2017.
- [9] F. Baccelli and B. Blaszczyszyn, *Stochastic Geometry and Wireless Networks, Volume I - Theory*. Now Publishers, 2009.
- [10] Cisco. WLAN Radio Frequency Design Considerations. [Online]. Available: <https://www.cisco.com/en/US/docs/solutions/Enterprise/Mobility/emb30d/RFDesign.html>
- [11] R. S. Sutton and A. G. Barto, *Intro. to Reinforcement Learning*, 1998.
- [12] S. Koenig and R. Simmons, "Complexity Analysis of Real-Time Reinforcement Learning," in *AAAI Conf. on Artif. Intelligence*, 1993.
- [13] L. Yamamoto and J. Beerends, "Impact of Network Performance Parameters on the End-to-End Perceived Speech Quality," in *Proc. of Expert ATM Traffic Symposium*, 1997.
- [14] J. Proakis, *Digital Communications*. McGraw-Hill, 2001.
- [15] F. B. Mismar. (2018) Deep Q -Learning Code. [Online]. Available: <https://github.com/available-after-review>
- [16] F. Chollet *et al.*, "Keras," 2015. [Online]. Available: <https://github.com/keras-team/keras>
- [17] M. Abadi, A. Agarwal, P. Barham, E. Brevdo, Z. Chen *et al.*,

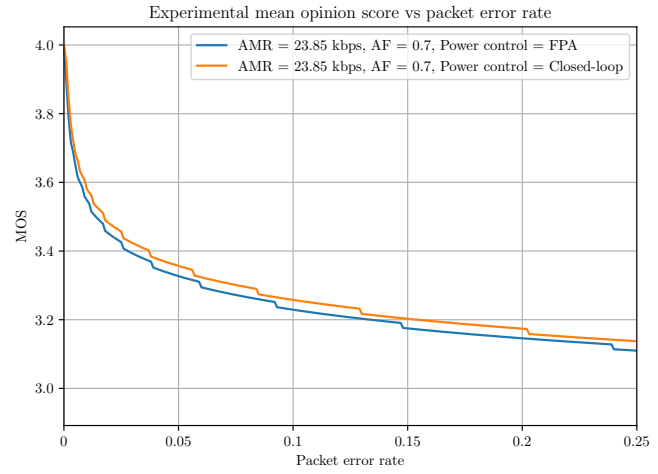


Fig. 9. Mean opinion score (MOS) based on the voice packet error rate and the experimental formula [13]. Closed-loop Q -Learning has improved MOS compared to Fixed Power Allocation (FPA).

“TensorFlow: Large-Scale Machine Learning on Heterogeneous Systems,” 2015. [Online]. Available: <https://www.tensorflow.org/>